THE JOURNAL OF PHYSICAL CHEMISTRY C

ARTICLE

pubs.acs.org/JPCC

CO Catalytic Oxidation on Copper-Embedded Graphene

E. H. Song, Z. Wen,* and Q. Jiang*

Key Laboratory of Automobile Materials, Ministry of Education, and Department of Materials Science and Engineering, Jilin University, Changchun 130022, China

ABSTRACT:

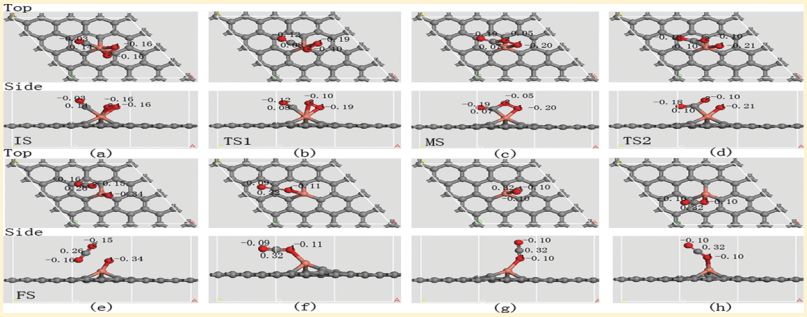

The catalytic oxidation of CO on Cu-embedded graphene is investigated by DFT. The reaction proceeds via a two-step mechanism of $CO + O_2 \rightarrow OOCO \rightarrow CO_2 + O$ and $CO + O \rightarrow CO_2$. The energy barriers of the former are 0.25 and 0.54 eV, respectively, while the latter is a process with energetic drop. The high activity of Cu-embedded graphene may be attributed to the electronic resonance among electronic states of CO, O_2, and the Cu atom, particularly among Cu-3d, CO-2π^*, and O_2-2π^* orbitals. This good catalytic activity opens a new avenue to fabricate carbon-based catalysts for CO oxidation with lower cost and higher activity.

1. INTRODUCTION

CO oxidation plays an important role in solving the growing environmental problems caused by CO emission from automobiles, industrial processes, and so on. Earlier investigations, both experimentally[1−5] and theoretically,[6−21] have been made to lower the energy barrier E_r values for CO oxidation on metallic surfaces. For examples, some noble metals of Pt,[1,2,6−9,17,18,21] Pd,[3,8,10,11,17,18,21] Rh,[4,8,12,13,17,18,20,21] Au,[5,14−16,19] etc., can effectively catalyze CO oxidation. They are however costly and require high reaction temperatures for efficient operations. In order to conquer this bottleneck, recent studies address novel catalysts such as alloys,[22−24] clusters,[25−32] metal oxides,[33,34] and even metallic nanotubes.[35] Obviously, catalysts with higher activity and lower cost are desirable for wide applications.

Graphene, a one-atom-thick carbon sheet with unique electronic and geometric properties, has been regarded as one of the most promising candidates for the next generation of electronic materials.[36−38] Recently, graphene has been extensively studied as a support for heterogeneous catalysts due to the huge surface-to-volume ratio for catalytic reaction,[39] such as Pt supported on graphene sheets,[40−42] Au- or Fe-embedded graphene,[43,44] TiO_2-decorated graphene,[45,46] and even intrinsic graphene under electric field.[47] Note that the metal-embedded graphene structures have been fabricated experimentally with good thermal stabilities[48] due to stronger bonding between metals and neighboring carbon atoms.[49−51] Thus, these investigations provide a comprehensive understanding that graphene may be a very active catalyst through the interactions between the carbon vacancies and metal clusters or a single atom.

On the basis of the above evidence, it is natural to expect that Cu-embedded graphene (Cu/graphene) can also exhibit a similar catalytic behavior since Cu and Au belong to the same elemental group of the noble metals with a similar electronic structure. In addition, Cu is cheap, environmentally benign, readily available, and rich in the earth, meeting our requirements to develop low-cost, green, and efficient catalysts. In this work, we investigate the catalytic oxidation of CO on Cu/graphene by means of the first-principle calculations. Our calculations suggest that Cu/graphene can also exhibit similar or even higher catalytic behavior like the Au/graphene and Fe/graphene systems.[43,44]

2. COMPUTATIONAL METHOD

All calculations were performed using the spin-unrestricted density functional theory (DFT) as implemented in the DMol^3 code.[52,53] Exchange-correlation functions were computed within a local density approximation with Perdew−Wang correlation (PWC).[54] DFT semicore pseudopotentials (DSPPs) core treatment[55] was implemented for relativistic effects, which replaced core electrons by a single effective potential. In addition, double numerical plus polarization (DNP) was chosen as the basis set and the quality of orbital cutoff is fine.

A hexagonal graphene supercell (4 × 4 graphene unit cell) containing 32 atoms was introduced to model a system where

Received: September 20, 2010
Revised: January 8, 2011
Published: February 11, 2011

ACS Publications © 2011 American Chemical Society

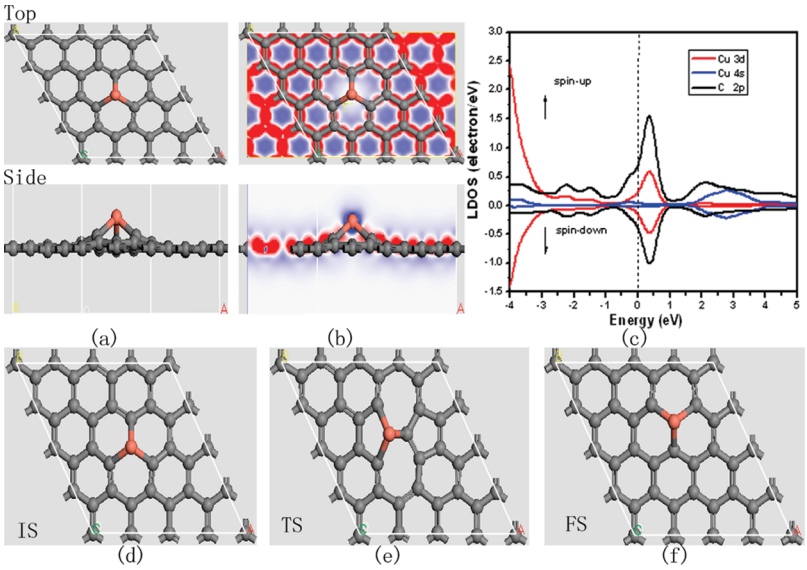

Figure 1. Top and side views of the geometric (a) and electronic (b) structures of Cu/graphene. The big jacinth (small gray) ball represents the Cu atom (carbon atoms). The red and blue regions show the electron accumulation and loss. (c) Spin-polarized local density of states projected on Cu-3d (red), Cu-4s (blue), and C-2p (black for neighboring carbon atoms) orbital curves. The Fermi level is set to zero. (d−f) Atomic configurations of the initial state (IS), transition state (TS), and final state (FS) for the migration of a Cu-vacancy pair in graphene sheet.

one C atom is substituted by a Cu atom, approaching the isolated impurity limit. The modulus unit cell vector in the z direction was set to 13 Å, which led to negligible interactions between the system and their mirror images. For geometric optimization and the search for the transition state (TS), the Brillouin zone integration was performed with $3 \times 3 \times 1$ k-point sampling, which brings out the convergence tolerance of energy of 1.0×10^{-5} hartree and that of maximum force of 0.002 hartree. For the density-of-states (DOS) calculation, the k-point was set to $20 \times 20 \times 1$ to achieve high accuracy. Charge transfers were calculated with the Hirshfeld charge analysis method.[56] To investigate the minimum energy pathway (MEP) for CO oxidation, linear synchronous transit (LST/QST) and nudged elastic band (NEB)[57] tools in DMol^3 code were used, which have been well validated to find TS and MEP. The adsorption energy E_{ad} between the adsorbate and Cu/graphene is defined as

$$E_{ad} = E_t - (E_{Cu/graphene} + E_{adsorbate}) \quad (1)$$

where the subscripts t, Cu/graphene, and adsorbate denote the total energies and the energies of the corresponding substances.

3. RESULTS AND DISCUSSION

Figure 1 shows the geometric and electronic properties of Cu-embedded graphene (Cu/graphene). The Cu atom is located on top of the single vacancy H site, forming three bonds with the nearest carbon atoms, as shown in Figure 1a. The bond length between Cu and neighboring C (l_{Cu-C}) is 1.83 Å, and the distance between Cu and the graphene sheet is 1.32 Å, which is a little smaller than that of literature data (about 1.7 Å).[50] This difference may be due to distinct exchange and correlation functions used. Meanwhile, there is about 0.37e charge transfer (Q) from Cu to graphene sheet according to the Hirshfeld charge population analysis, and the magnetic moment of the whole system is 0.93 μ_B compared with the literature data of about 1.3 μ_B.[50] The charge transfer can also be verified by the difference of electronic densities of Cu/graphene, as shown in Figure 1b where the red and blue regions represent the areas of electron accumulation and loss, respectively. Obviously, different electron affinities of Cu and C change the electron distribution of the Cu/graphene system. However, the whole graphene structure remains covalent in nature due to the electrons are mainly located within the bonds rather than heavily centered on the C atoms, as shown the top view of Figure 1b.

To gain deeper insight into the electron structure of Cu/graphene, the spin-polarized local density of states projected on Cu-3d and Cu-4s orbitals and neighboring C-2p orbital is plotted, as shown in Figure 1c. Because of the formation of C−Cu bonds and charge transfer from Cu to C, Cu-4s, Cu-3d, and C-2p orbitals are partially filled. As a result, the high density of spin-polarized states is localized around E_F while the localized Cu-3d orbital is important to activate reactants to lower the reaction barriers, which will be discussed later.

Considering the possible clustering problem of Cu atom embedded graphene, we also computed the energy barrier for Cu diffusion in graphene from the vacancy site H to its neighboring one. Parts d and f of Figure 1 show the initial and final structures, respectively, where the Cu-vacancy pair moves or migrates to a neighboring site. One C bond breaks first, and a pentagon forms during the migration (Figure 1e). The diffusion energy barrier E_r is ∼2.34 eV, which implies that metal clustering problem is absent and the Cu/graphene system is the energetically stable structure. Therefore, we can deduce that the carbon vacancies or dangling bonds of carbon atoms can improve the stability of Cu atom on graphene and tune the electronic structure of Cu atom.

Herein, we first consider the adsorptions of CO and O_2 with Cu/graphene, respectively. Figure 2a shows the most stable end-on configuration of CO on Cu/graphene system with E_{ad}(CO) = −1.71 eV. Meanwhile, there is about 0.02e charge transfer from Cu/graphene to CO, which occupies CO-2π^* orbital and subsequently leads to the elongation of l_{C-O} from 1.13 to 1.15 Å (Figure 2b,c). In this case, the electrons not only accumulate on O ion but also on C−Cu bond. However, the whole graphene

dx.doi.org/10.1021/jp108978c |J. Phys. Chem. C 2011, 115, 3678–3683

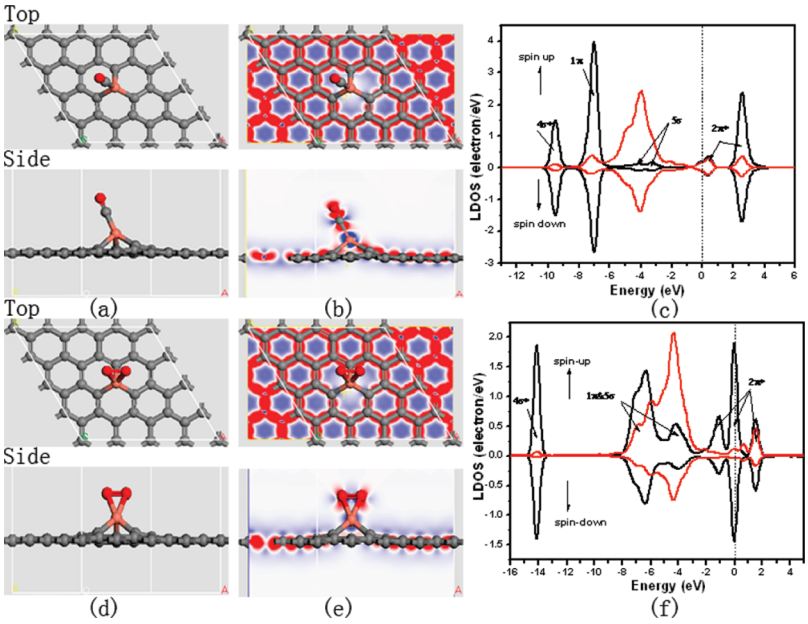

Figure 2. Top and side views of the geometric (a, d) and electronic (b, e) structures of CO and O_2 adsorbed on Cu/graphene, respectively. (c) Spin-polarized local density of states projected onto CO on Cu/graphene. Red and black curves indicate the d-projected LDOS of Cu and the adsorbed CO, respectively. (f) Spin-polarized local density of states projected onto O_2 on Cu/graphene. Black curve shows adsorbed O_2.

structure remains covalent, shown in the top view of Figure 2b. The strong hybridization between Cu-3d and CO-2π^* orbitals is observed near E_F from the computed DOS (Figure 2c). This also indicates that the variation in bond strength is caused by CO 2π^*-d coupling; namely, the stronger this coupling, the stronger the CO−metal bonding.[58] For the Cu/graphene system, CO adsorption increases the magnetic moment of the whole system to 0.94 μ_B, which is induced by the increase of unpaired electron numbers due to the hybridization between Cu and C atoms.

For O_2 adsorption on Cu/graphene, the most energetically favorable configuration is characterized by O_2, being parallel to the graphene sheet and forming two chemical bonds with Cu (side on) where $E_{ad}(O_2) = -2.67$ eV, which is more favorable than the end-on configuration of CO (Figure 2d). There is about 0.30e charge transfer from Cu/graphene to O_2, which occupies O_2-2π^* orbital and brings out l_{O1-O2} elongation from 1.21 to 1.35 Å, as shown in Figure 2e,f. In this case, the electrons mainly accumulate on O_2 where O_2-2π^* orbital is half-filled, and the whole graphene structure is still covalent. Similar to O_2 adsorbed on Mn/graphene system,[59] O_2 adsorption with the hybridization between Cu and O atoms reduces the magnetic moment of whole system to 0.53 μ_B due to the drop of unpaired electron numbers.

Since O_2 interacts with Cu/graphene stronger than CO, Cu of Cu/graphene should be covered by O_2 if CO and O_2 are coadsorbed, which is also an exothermic process with $E_{ad}(CO+O_2) = -3.29$ eV, being larger than $E_{ad}(CO)$ and $E_{ad}(O_2)$. In fact, a stronger binding strength between the adsorbates and the catalyst may promote associated product formation.[43,44] Meanwhile, there is about 0.21e charge transfer (Q) from Cu/graphene sheet to CO + O_2, and the magnetic moment of the whole system is a 0.33 μ_B. In addition, the most stable adsorption site of CO_2 locates on Cu (end-on configuration) with $E_{ad}(CO_2) = -0.49$ eV via researching various possible adsorption sites, suggesting a weak adsorption of CO_2 on Cu/graphene and can easily desorb from the reaction site.

There are two well-established reaction mechanisms [Langmuir−Hinshelwood (LH) and Eley−Rideal (ER)] between adsorbed CO and O_2.[29,35,43,44] We find that the dissociative adsorption of O_2 on Cu atom is energetically unfavorable when O_2 interacts with the Cu/graphene system. Thus, the ER mechanism is hardly possible in our case as a starting point, which is similar to the case of CO oxidation on Au/graphene system.[43] Let the LH reaction of CO + O_2 → OOCO → CO_2 + O as a starting point; the ER reaction of CO + O → CO_2 is followed. To search for the minimum-energy pathway (MEP) for CO oxidation, we selected the most stable coadsorption configuration as an initial state (IS), where CO and O_2 are tilted and parallel to the graphene sheet, respectively (Figure 3a). The final state (FS) consists of a CO_2 molecule physisorbed on Cu/graphene with a chemisorbed atomic O nearby (Figure 3e). The local configurations of the adsorbates on Cu/graphene at each state along MEP are also displayed in Figure 3.

Once CO and O_2 are coadsorbed on Cu/graphene, one oxygen atom O2 approaches C of CO and reaches TS1. The energy barrier E_r along MEP is estimated to be 0.25 eV. Meanwhile, a peroxo-type O1−O2−C−O complex is formed above Cu atom. Passing over TS1, the complex is still maintained until a metastable configuration (MS1) is reached. Meanwhile, there is about 0.37e charge transfer from Cu/graphene sheet to O1−O2−C−O complex, and the size of the magnetic moment of the whole system is 0.12 μ_B. The bond length l_{O1-O2} increases from 1.35 to 1.47 Å in this exothermic process. The reaction continuously proceeds from MS1 to FS with a relatively high E_r value of 0.54 eV (TS2) where CO_2 is formed, leaving an atomic O1 adsorbed on Cu/graphene. There is about 0.39e charge transfer from Cu/graphene sheet to O1 (0.34e) and CO_2 (0.05e), and the magnetic moment of whole system is nearly zero. We conclude that the magnetization of the whole system almost vanishes after CO_2 and O are adsorbed on Cu/graphene.

In the catalysis theory, it is known that the overall barrier is important rather than a particular barrier. Usually, if one of

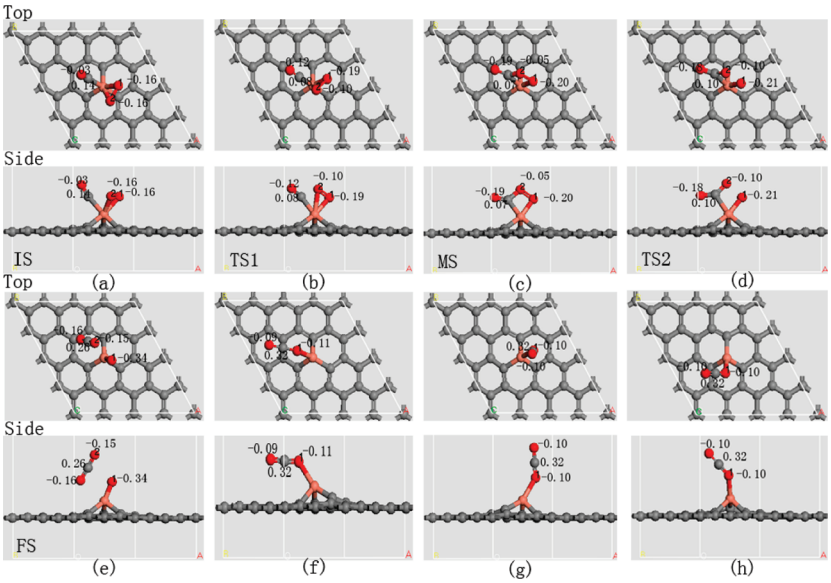

Figure 3. Local configurations of the adsorbates on Cu/graphene at each state along MEP. In the first step, corresponding structures include IS (a), TS1 (b), MS (c), TS2 (d), and FS (e) along MEP via the CO + O_2 → OOCO → CO_2 + O route. In the second step, the corresponding final structures include three binding sites (parallel, perpendicular, tilted) for CO_2 adsorbed on Cu/graphene via CO + O → CO_2 route (f–h).

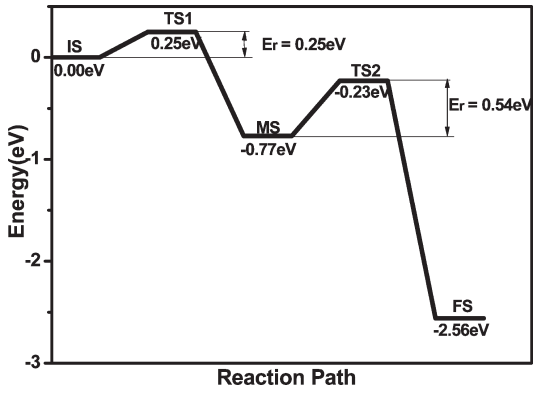

Figure 4. Schematic energy profile corresponding to local configurations shown in Figure 3a–e along the minimum-energy pathway via the CO + O_2 → OOCO → CO_2 + O route. All energies are given with respect to the reference energy.

intermediate reactions is endothermic, the overall barrier can be higher than all the particular ones. Otherwise, the overall barrier should be equal to the highest particular one. To clarify the barrier case, the MEP profile is also summarized in Figure 4 where the schematic energy profile corresponds to local configurations shown in Figure 3a–e along the minimum-energy pathway via the CO + O_2 → OOCO → CO_2 + O route. As shown in Figure 4, both the intermediate and final reactions of CO + O_2 → OOCO → CO_2 + O are exothermic with particular barriers of 0.25 and 0.54 eV. Thus, the overall barrier should be equal to the latter one, namely 0.54 eV.

We also checked whether CO oxidation with atomic O1 (ER mechanism) is conceivable after CO_2 is formed via ER mechanism. We first chose three configurations (parallel, perpendicular, tilted) of the CO molecule more than 3.0 Å away from the atomic O1 preadsorbed on Cu, followed by the step that O1 bound with Cu reacts with CO to produce CO_2. It was found that the reactions can proceed without energy barriers, namely, CO is easily adsorbed on the O/Cu/graphene system (Figure 3f–h). Note that the largest E_{ad} value of CO_2 on Cu/graphene is only −0.49 eV. Thus, CO_2 can be easily desorbed from Cu/graphene system due to the weak adsorption. Comparing with several previous works, we found that the largest E_r = 0.54 eV is much lower than those of commonly used catalysts such as Pt,[1,2,6−9,17,18,21] Pd,[3,8,10,11,17,18,21] Rh,[4,8,12,13,17,18,20,21] Au,[5,14−16,19] etc., merely around 1.00 eV. Note that the values for Au/graphene and Fe/graphene systems are 0.31 and 0.58 eV.[43,44] Moreover, the second step of the oxidation on Cu/graphene (the Eley–Rideal reaction) proceeds without energy barrier while the reported lowest magnitude of E_r value is 0.03 eV for CO oxidation with atomic O on Au nanotube.[35]

To gain more insight into the origin of the high activity of Cu/graphene system, we investigate the electronic structures in LH reaction progresses. As we discussed above, the partially occupied Cu-3d orbital, being crucial for the activity, is localized around E_F due to the interaction between Cu and graphene. Figure 5 shows the electronic local density of states (LDOS) projected onto C–O and O1–O2 bonds as well as the d-projected LDOS of Cu in IS, TS1, MS, and TS2 of LH step, respectively. The s- and p-projected LDOS of Cu and p-projected LDOS of C have no significant change in the reaction progresses and are thus not shown here. Up on CO and O_2 coadsorption, the Cu-3d orbital is partially occupied in IS configuration with the charge transfer between Cu and adsorbates. The antibonding orbitals of CO-2π^* and O_2-2π^* are partially filled due to the strong hybridization with the Cu-3d orbital. In addition, 1π and 5σ orbitals of CO and O_2 are more broadened and involved with Cu-3d orbital, compared with Figure 2c,f. From IS to TS1, O_2-1π and O_2-2π^* orbitals are gradually broadened and involved within Cu-3d orbitals to weaken the O1–O2 bond. In the MS, the strong hybridization between 1π and 5σ orbitals of O_2 and Cu-3d orbital can be observed below the Fermi level. From MS to TS2, the occupied 2π^* orbital is elevated above E_F due to the interaction between O2 and CO mediated by Cu, as indicated by the decrease of l_{C-O2}. As comparisons, 4σ^* orbital is not involved in the reaction

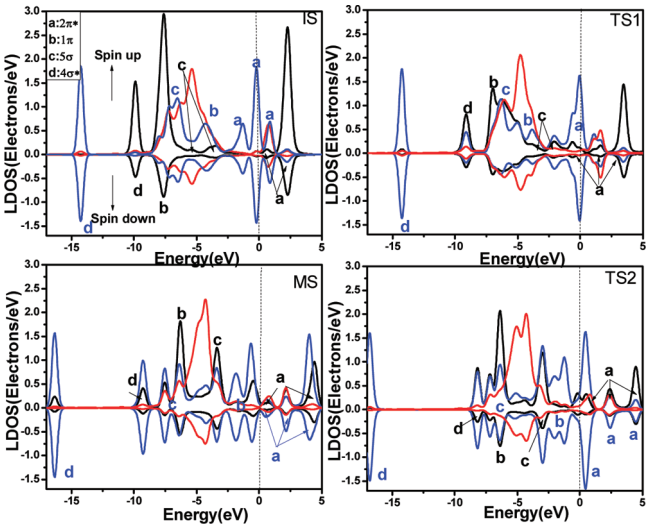

Figure 5. Spin-polarized local density of states (LDOS) projected onto C−O and O1−O2 on the Cu/graphene (Figure 3a−e), together with the d-projected LDOS of the Cu atom in the IS, TS1, MS, and TS2. Black solid curve, C−O on Cu/graphene; blue solid curve, O1−O2 on Cu/graphene; red curve, d-projected LDOS of the Cu atom. The Fermi level is set to zero. The orbital notations are roughly indicated by a, b, c, and d in reaction processes.

since its position is far below E_F. For C−O species on Cu/graphene, 1π and 5σ orbital, below E_F, is strongly hybridized with Cu-3d orbital in IS. The CO-$2\pi^*$ orbital is also pulled close to E_F, and it is partially filled due to the electronic resonance between C−O-$2\pi^*$ and Cu-3d orbitals from IS to TS1. From MS to TS2, the $2\pi^*$ state of C−O is gradually elevated above E_F. The partial occupation of this antibond leads to the slight increase of C−O bond length (MS) and finally reduces the C−O bond length close to the value of l_{C-O} of an isolated CO_2 molecule. A net charge transfer from Cu to the adsorbates in these reaction progresses occurs, resulting in partially filled Cu-3d orbital. Overall, the formation of the unstable peroxo-type O1−O2−C−O complex results in a redistribution of LDOS and an orbital shift for both C−O and O1−O2 species. From IS to TS1 to MS to TS2, the C−O-$2\pi^*$ and O1−O2-$2\pi^*$ orbitals are expanded and involved with the Cu-3d orbital. Moreover, mediated by Cu, the states of C−O and O1−O2 interact with each other, strengthening C−O2 bond while weakening O1−O2 bond, as indicated by the superposition of the C−O and O1−O2 states at TS2. Meanwhile, Cu-3d orbital dominates the interaction between CO and O_2 on the Cu/graphene system. For ER reaction, Cu is positively charged due to the higher electronegativity of O1 prebonded with Cu. The Cu-3d orbital is partially filled while CO approaches O1 directly and forms C−O1 bond.

In light of the above discussion, we conclude that CO oxidation on Cu/graphene may be characterized as a two-step process: LH reaction initiates CO oxidation with E_r = 0.25 eV and E_r = 0.54 eV followed by ER reaction without energy barrier. The both reaction steps could proceed rapidly because of the low E_r values involved.

4. CONCLUSION

In summary, we performed DFT calculations to investigate the reaction mechanism of CO oxidation catalyzed by the Cu/graphene system as well as structural and electronic properties of adsorbates and adsorbents. We found that the system has a high catalytic activity via the oxidation reaction of CO molecule. CO oxidation most likely proceeds with LH reaction as the starting point with lower activation barriers of 0.25 and 0.54 eV, followed by ER reaction without energy barrier. The high activity of Cu/graphene may be attributed to the electronic resonance among electronic states of CO, O_2, and the Cu atom, particularly, among Cu-3d, CO-$2\pi^*$, and O_2-$2\pi^*$ orbitals. This good catalytic activity shows that Cu/graphene system is a good candidate for CO oxidation with lower cost and higher activity.

AUTHOR INFORMATION

Corresponding Author

*E-mail wenzi@jlu.edu.cn (Z.W.), jiangq@jlu.edu.cn (Q.J.); Tel +86 431 85095371; Fax +86 431 85095876.

ACKNOWLEDGMENT

We acknowledge support by National Key Basic Research, Development Program (Grant No. 2010CB631001), and by Program for Changjiang Scholars and Innovative Research Team in University and High Performance Computing Center (Jilin University).

REFERENCES

(1) Ackermann, M. D.; Pedersen, T. M.; Hendriksen, B. L. M.; Robach, O.; Bobaru, S. C.; Popa, I.; Quiros, C.; Kim, H.; Hammer, B.; Ferrer, S.; Frenken, J. W. M. *Phys. Rev. Lett.* **2005**, *95*, 255505.
(2) Nakai, I.; Kondoh, H.; Amemiya, K.; Nagasaka, M.; Nambu, A.; Shimada, T.; Ohta, T. *J. Chem. Phys.* **2004**, *121*, 5035.
(3) Nakai, I.; Kondoh, H.; Shimada, T.; Resta, A.; Andersen, J. N.; Ohta, T. *J. Chem. Phys.* **2006**, *124*, 224712.
(4) Krenn, G.; Bako, I.; Schennach, R. *J. Chem. Phys.* **2006**, *124*, 144703.
(5) Kimble, M. L.; Castleman, A. W.; Mitrić, R.; Bürgel, C.; Bonačić-Koutecký, V. *J. Am. Chem. Soc.* **2004**, *126*, 2526.
(6) Alavi, A.; Hu, P.; Deutsch, T.; Silvestrelli, P. L.; Hutter, J. *Phys. Rev. Lett.* **1998**, *80*, 3650.
(7) Eichler, A.; Hafner, J. *Surf. Sci.* **1999**, *435*, 58.
(8) Eichler, A. *Surf. Sci.* **2002**, *498*, 314.
(9) Bleakley, K.; Hu, P. *J. Am. Chem. Soc.* **1999**, *121*, 7644.
(10) Zhang, C. J.; Hu, P. *J. Am. Chem. Soc.* **2001**, *123*, 1166.
(11) Salo, P.; Honkala, K.; Alatalo, M.; Laasonen, K. *Surf. Sci.* **2002**, *516*, 247.
(12) Sljivancanin, Z.; Hammer, B. *Phys. Rev. B* **2010**, *81*, 121413.
(13) Liu, D. J. *J. Phys. Chem. C* **2007**, *111*, 14698.
(14) Socaciu, L. D.; Hagen, J.; Bernhardt, T. M.; Wöste, L.; Heiz, U.; Häkkinen, H.; Landman, U. *J. Am. Chem. Soc.* **2003**, *125*, 10437.
(15) Lopez, N.; Nørskov, J. K. *J. Am. Chem. Soc.* **2002**, *124*, 11262.
(16) Liu, Z. P.; Hu, P.; Alavi, A. *J. Am. Chem. Soc.* **2002**, *124*, 14770.
(17) Chen, M. S.; Cai, Y.; Yan, Z.; Gath, K. K.; Axnanda, S.; Goodman, D. W. *Surf. Sci.* **2007**, *601*, 5326.
(18) Oh, S.-H.; Hoflund, G. B. *J. Catal.* **2007**, *245*, 35.
(19) Kandoi, S.; Gokhale, A. A.; Grabow, L. C.; Dumesic, J. A.; Mavrikakis, M. *Catal. Lett.* **2004**, *93*, 93.
(20) Stampfl, C.; Scheffler, M. *Surf. Sci.* **1999**, *433*, 119.
(21) Liu, W.; Zhu, Y. F.; Lian, J. S.; Jiang, Q. *J. Phys. Chem. C* **2006**, *111*, 1005.
(22) Zhang, C. J.; Baxter, R. J.; Hu, P.; Alavi, A.; Lee, M.-H. *J. Chem. Phys.* **2001**, *115*, 5272.
(23) Liu, X.; Wang, A.; Wang, X.; Mou, C. Y.; Zhang, T. *Chem. Commun.* **2008**, 3187.
(24) Dupont, C. l.; Loffreda, D.; Delbecq, F. o.; Santos Aires, F. J. C.; Ehret, E.; Jugnet, Y. *J. Phys. Chem. C* **2008**, *112*, 10862.

(25) Wallace, W. T.; Whetten, R. L. *J. Am. Chem. Soc.* **2002**, *124*, 7499.
(26) Chang, C. M.; Cheng, C.; Wei, C. M. *J. Chem. Phys.* **2008**, *128*, 124710.
(27) Okamoto, Y. *Chem. Phys. Lett.* **2006**, *420*, 382.
(28) Liu, W.; Zhao, Y. H.; Zhang, R. Q.; Li, Y.; Lavernia, E. J.; Jiang, Q. *ChemPhysChem* **2009**, *10*, 3295.
(29) Molina, L. M.; Hammer, B. *J. Catal.* **2005**, *233*, 399.
(30) Gao, Y.; Shao, N.; Bulusu, S.; Zeng, X. C. *J. Phys. Chem. C* **2008**, *112*, 8234.
(31) Gao, Y.; Shao, N.; Pei, Y.; Zeng, X. C. *Nano Lett.* **2010**, *10*, 1055.
(32) Du, J.; Wu, G.; Wang, J. *J. Phys. Chem. A* **2010**, *114*, 10508.
(33) Gong, X.-Q.; Liu, Z.-P.; Raval, R.; Hu, P. *J. Am. Chem. Soc.* **2003**, *126*, 8.
(34) Molina, L. M.; Hammer, B. *Phys. Rev. Lett.* **2003**, *90*, 206102.
(35) An, W.; Pei, Y.; Zeng, X. C. *Nano Lett.* **2008**, *8*, 195.
(36) Geim, A. K. *Science* **2009**, *324*, 1530.
(37) Rao, C. N. R.; Sood, A. K.; Subrahmanyam, K. S.; Govindaraj, A. *Angew. Chem., Int. Ed.* **2009**, *48*, 7752.
(38) Ratinac, K. R.; Yang, W.; Ringer, S. P.; Braet, F. *Environ. Sci. Technol.* **2010**, *44*, 1167.
(39) Boukhvalov, D. W.; Katsnelson, M. I. *J. Phys. Chem. C* **2009**, *113*, 14176.
(40) Yoo, E. J.; Okata, T.; Akita, T.; Kohyama, M.; Nakamura, J.; Honma, I. *Nano Lett.* **2009**, *9*, 2255.
(41) Seger, B.; Kamat, P. V. *J. Phys. Chem. C* **2009**, *113*, 7990.
(42) Tanaka, K.-i.; Shou, M.; Yuan, Y. *J. Phys. Chem. C* **2010**, *114*, 16917.
(43) Lu, Y. H.; Zhou, M.; Zhang, C.; Feng, Y. P. *J. Phys. Chem. C* **2009**, *113*, 20156.
(44) Li, Y.; Zhou, Z.; Yu, G.; Chen, W.; Chen, Z. *J. Phys. Chem. C* **2010**, *114*, 6250.
(45) Williams, G.; Seger, B.; Kamat, P. V. *ACS Nano* **2008**, *2*, 1487.
(46) Zhang, X. Y.; Li, H. P.; Cui, X. L.; Lin, Y. H. *J. Mater. Chem.* **2010**, *20*, 2801.
(47) Ao, Z. M.; Peeters, F. M. *Appl. Phys. Lett.* **2010**, *96*, 253106.
(48) Gan, Y.; Sun, L.; Banhart, F. *Small* **2008**, *4*, 587.
(49) Malola, S.; Hakkinen, H.; Koskinen, P. *Appl. Phys. Lett.* **2009**, *94*, 043106.
(50) Krasheninnikov, A. V.; Lehtinen, P. O.; Foster, A. S.; Pyykko, P.; Nieminen, R. M. *Phys. Rev. Lett.* **2009**, *102*, 126807.
(51) Zhang, W.; Sun, L.; Xu, Z.; Krasheninnikov, A. V.; Huai, P.; Zhu, Z.; Banhart, F. *Phys. Rev. B* **2010**, *81*, 125425.
(52) Delley, B. *J. Chem. Phys.* **1990**, *92*, 508.
(53) Delley, B. *J. Chem. Phys.* **2000**, *113*, 7756.
(54) Perdew, J. P.; Wang, Y. *Phys. Rev. B* **1992**, *45*, 13244.
(55) Delley, B. *Phys. Rev. B* **2002**, *66*, 155125.
(56) Hirshfeld, F. L. *Theor. Chim. Acta* **1977**, *44*, 129.
(57) Henkelman, G.; Jonsson, H. *J. Chem. Phys.* **2000**, *113*, 9978.
(58) Crawford, P.; Hu, P. *J. Phys. Chem. B* **2006**, *110*, 24929.
(59) Dai, J.; Yuan, J. *Phys. Rev. B* **2010**, *81*, 165414.